Edinburgh Research Explorer

Human in the loop heterogeneous modelling of thermostatically 1 controlled loads for Demand Side Management studies.

OPEN ACCESS
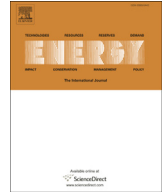
Human in the loop heterogeneous modelling of thermostatically controlled loads for demand side management studies

Alexandros Kleidaras, Aristides E. Kiprakis[*], John S. Thompson

School of Engineering, University of Edinburgh, EH9 3DW, Edinburgh, UK

A B S T R A C T

Demand Response (DR) is a Smart Grid technology aiming to provide demand regulation for dynamic pricing and ancillary services to the grid. Thermostatically controlled loads (TCLs) are among those with the highest potential for DR. Some of the challenges in modelling TCLs is the various factors that affect their duty cycle, mainly human behaviour and external conditions, as well as heterogeneity of TCLs (load parameters). These add an element of stochasticity, with detrimental impact on the aggregated level. Most models developed so far use Wiener processes to represent this behaviour, which in aggregated models, such as those based on Coupled Fokker-Planck Equations (CFPE), have a negligible effect as "white noise". One of the main challenges is modelling the effect of external factors on the state of TCLs' aggregated population and their impact in heterogeneity during operation. Here we show the importance of those factors as well as their detrimental effect in heterogeneity using cold loads as a case study. A bottom up detailed model has been developed starting from thermal modelling to include these factors, real world data was used as input for realistic results. Based on those we found that the duty cycle of some TCLs in the population can change significantly and thus the state of the TCLs' population as a whole. Subsequently, the accuracy of aggregation models assuming relative homogeneity and based on small stochasticity (i.e. Wiener process with typical variance 0.01) is questionable. We anticipate similar realistic models to be used for real world applications and aggregation methods based on them, especially for cold loads and similar TCLs, where external factors and heterogeneity in time are significant. DR control frameworks for TCLs should also be designed with that behaviour in mind and the developed bottom up model can be used to evaluate their accuracy.

© 2018 The Authors. Published by Elsevier Ltd. This is an open access article under the CC BY license (http://creativecommons.org/licenses/by/4.0/).

1. Introduction

As more intermittent renewable and distributed energy comes onto the grid, old generation resources are retired and costly new plant expenditures are avoided. Transmission congestion in Medium Voltage and Low Voltage becomes a larger problem [1], and therefore new Demand Response (DR) programs are emerging. Economic optimization under dynamic pricing, as well as provision of ancillary services and regulation through DR has been in the spotlight of Smart Grid research [2,3]. Balancing demand and supply has predominantly been achieved by supply regulation, but in some cases by demand regulation too. Theoretically any regulation measure from the "supply side" has an equivalent

countermeasure from the "demand side". In practice, generation units have different characteristics than loads, and DR consequently has to be engaged as such, thus examine DR's suitability for ancillary services and form regulations specifically for DR. It is imperative to note that DR comes from aggregation of large populations of loads with different characteristics. It would be challenging to track the state of each one in real time, but estimating the state of the population probabilistically is possible and can be accurate [4]. Moreover, based on the type of loads aggregated, there are different characteristics of the population; accordingly, constraints and potential for ancillary services of each population. The problem of aggregation and scalability is one of the major challenges DR faces, whose potential solution could be clustering, a topic discussed in this paper and will be examined more in depth in future work. DR programs (mainly from industrial units) provide ancillary services [6] or regulation [7] and can replace wholly or partial conventional units; commercial and residential DR services are under development and have relatively low enrolment to date [5]. Basic types of

* Corresponding author.
E-mail addresses: A.Kleidaras@ed.ac.uk (A. Kleidaras), Aristides.Kiprakis@ed.ac.uk (A.E. Kiprakis), John.Thompson@ed.ac.uk (J.S. Thompson).

Nomenclature		C	Thermal capacitance kWh/°C
		R	Thermal resistance °C/kW
θ	Temperature (°C)	c	Cooling rate
θ_a	Ambient temperature (°C)	r	Heating rate
θ_{set}	Set temperature (°C)	t_{on}	Time in ON state (minutes)
θ_g	Temperature gain in ON state (°C)	t_{idle}	Time in OFF/idle state (minutes)
δ	temperature deadband	T	Cycle period ($t_{on} + t_{idle}$)
R	Thermal Resistance (°C/kW)	D	Duty cycle (t_{on}/T)
P	Power Rate (Watts)	N	Number of TCLs
m	1 for ON state, 0 for OFF/idle state	Q	Heat flux
W	Wiener process	u	1 for external interaction (0 otherwise)
l	Time step	λ	Heat transfer coefficient (W/(m²K))

DR services can be seen in Fig. 1.

Not only can DR substitute conventional units for ancillary services, but they also bring several advantages including lower cost, no CO_2 emissions, instantaneous response [6], ability to reduce load peaks [8] and synergetic potential with Renewable Energy Sources (RES) intermittence [9]. Additionally, unique characteristics of DR can change the way balancing services work today. DR comes from loads, which are ubiquitous throughout the grid, giving the unique ability of spatial actions. Large distributed populations also have inherently higher reliability than conventionally units, in case an individual conventional unit becomes unavailable there is a great impact in overall availability. In addition, contingencies can be countered through DR, through grid relief, whilst a generation unit cannot provide such service. Modern approaches include "third party" aggregators, such as the OpenADR, originally developed at Lawrence Berkeley National Laboratory (LBNL), Berkley, CA [10]. The OpenADR Alliance formed in 2010, is an example of successful aggregated DR implementation with over 130 member companies (as of May 2016). Unfortunately, though, current implementations are unsophisticated regarding the impact to consumers. As the community has stated, with new AMI being deployed access to DR is inexpensive and what separates us from realising the full potential of DR is development of proper load models and their control strategies [11]. This paper focuses on examining the importance of external factors and creating a realistic model using cold loads as a case study.

A lot of effort has been focused on TCLs, due to the fact that they consume a large portion of the total electrical energy, in some buildings 40%–50% [7,12], while cold loads contribute 25%–36% of domestic consumption in UK [13]. TCLs are the most ubiquitous type of load, and especially in the case of cold loads they are plugged in 24/7, with the highest availability time wise [13]. On the other hand, when electric loads are used for space heating and cooling (i.e. air conditioners), they are usually one of the main sources of peaks in demand. Prediction of load dynamics is essential for DR optimization, both non-dispatchable and dispatchable, hence for power systems cost and reliability. For load forecasting purposes and energy efficiency, regression methods [14,15], can successfully be applied. Yet, prove inadequate for precise control of

TCLs and similar loads (refrigeration, electric space and/or water heating, air conditioners, heat pumps, electric vehicles etc.), which is essential for ancillary services such as provision of secondary frequency control or short term operating reserve [2]. DR actions alter demand out of its "ordinary" state, thus rendering past load measurements at best marginally useful, even more so in the case of dispatchable DR for emergencies (i.e. reserve, frequency control) [16]. Additionally, load behaviour and rebound effects at recovery time are not captured by forecasting models [16]. The model developed in this work is applicable to all TCLs, the focus is on DR for ancillary services, though it might also be used alongside regression models for faulty operation detection or energy efficiency. We choose cold loads for simulations and case studies as one of the most suitable type of TCLs.

Older DR concepts predefine aggregated load trajectory by suggesting load interruption [7,17], which causes consumer discomfort and risks withdrawal from participation in DR. Even those who do, such as fuzzy logic-based approaches for ancillary services [18] or peak load shaving and operating cost reduction [19], do not take into account the realistic limits of TCLs due to thermal characteristics. In addition, rebound effects were not taken into consideration.

Therefore, more sophisticated models have been favoured for TCLs, where thermal models are used extensively. Totu et al. [20] use a stochastic hybrid system for individual loads and a system of CFPE to describe the aggregated population, in order to develop a control algorithm for the aggregated population. The same individual modelling is used by Callaway [21], who focuses on finding the exact solution of the CFPE for homogeneous TCLs. In Ref. [22], Koch et al. a different modelling approach is considered, through stored thermal energy, and concludes in similar first order stochastic equations. This TCL model (or variations of it) has been used by the majority, whilst the main effort has been on obtaining more accurate aggregation methods or on control theory, such as Perfumo's et al. model-based control [23], or in Callaway's aggregation through CFPE [6,24], or Mathieu's et al. Markov Chain aggregation and control method [9] to name a few. A comparison of the main methods in summarized in Ref. [25]. It is important to note, that the above mention TCL model originates from Mortensen and Haggerty's work [26]; in general models described by Stochastic Partial Deferential Equations (S-PDE). The purpose of it was to study the "cold load pick up" phenomenon, for specific moments of the day, thus "static" conditions at those given moments. In Malhamé and Chong's work [27], it was proved that it is possible to construct a system of CFPE (equation (5) and (6)) to describe the aggregated behaviour of TCL populations for specific point in time, based on a few assumptions. Basic assumptions are: a) the load groups are homogeneous, b) there is no significant change in ambient
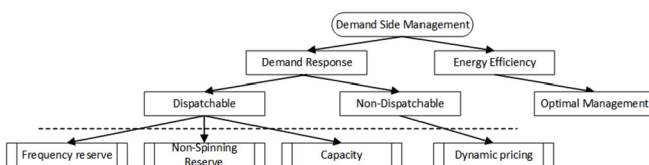

Fig. 1. Basic Demand Side Management services.

temperature in short periods and c) the above S-PDE does indeed represent the population and its behaviour accurately. More recently, Callaway went a step ahead [21], giving an exact solution to the CFPE, which provides the eigenvalues governing transient deviations from the steady state temperature distribution. Additionally, showing that small heterogeneity (described as "relative homogeneity" in this paper) within the population does actually improve the behaviour of the linear TCL model and associated control strategies, but for high heterogeneity renders the model inadequate. Those assumptions and points were the motivation for this paper. The main equation (1) has 3 basic parts; the (simplified) time varying solution of the differential equation that governs heat transfer mechanics (Newton's law of cooling), a discrete state varying parameter denoting the switch on/off state of TCLs and a stochastic part, commonly a Wiener process (Gaussian with mean 0, variance σ typically around $0.01°Cs^{-1/2}$ or similar distributions).

$$\theta_{i,t(n+1)} = \gamma_i \cdot \theta_{i,t(n)} + (1 - \gamma_i)\left[\theta_{a,i} - m_{i,t(n)} \cdot R_i \cdot P_i\right] + W_{i,t(n)}, \quad (1)$$

$$m_{i,t(n+1)} = \begin{cases} 0, \theta_{i,t(n)} < \theta_{set,i} - \dfrac{\delta_\iota}{2} = \theta_{min,i} \\ 1, \theta_{i,t(n)} > \theta_{set,i} + \dfrac{\delta_\iota}{2} = \theta_{max,i} \\ m_{i,tn}, otherwise \end{cases} \quad (2)$$

$$P_{total(n+1)} = \sum_1^N \frac{1}{\eta_\iota} P_i m_{i,t(n+1)} \quad (3)$$

$$\gamma_i = e^{-l/CR}, l = t_{n+1} - t_n \quad (4)$$

Annotation: θ temperature (°C), m switch state {0,1} [21], W Wiener process (Gaussian distribution with variance $h\sigma^2$), P power rate (Watts), C thermal capacitance (kWh/°C) and R thermal resistance (°C/kW), θ_s set-point temperature, δ width of temperature deadband, θ_{min} minimum (switch OFF) temperature, θ_{max} maximum (switch ON) temperature, η efficiency coefficient, l time step.

The main equations of Malhamé and Chong [27], as used by Callaway [21], can be written in continuous time for cooling/cold loads as:

$$\frac{\partial f_1}{\partial t} = \frac{\partial}{\partial t}\left[\left(\frac{1}{CR}(\theta(t) - \theta_a) + \frac{P}{C}\right)f_1\right] + \frac{\sigma^2}{2}\frac{\partial^2}{\partial \theta^2}f_1, \quad (5)$$

$$\frac{\partial f_0}{\partial t} = \frac{\partial}{\partial t}\left[\left(\frac{1}{CR}(\theta(t) - \theta_a)\right)f_0\right] + \frac{\sigma^2}{2}\frac{\partial^2}{\partial \theta^2}f_0, \quad (6)$$

Where $f_0(\theta, t)$ and $f_1(\theta, t)$ are the probability densities of loads in the off and on state respectively. At this point there are some important notes, the above are true for a homogenous (or almost homogeneous) population, θ_α is constant (or almost constant) and σ takes small values (i.e. 0.1 °C [16,21]) whilst being critical in determining the reaction of the population as stated by Malhamé & Chong [27]. This Wiener process is mainly used to model "random" factors (i.e. cold loads temperature change, door opening etc.) affecting the operation of TCLs, with mean value 0 and small variance. The argument here is whether a Wiener process is adequate for such modelling and if the above equations, as well as the following (equation (7) and (8)), hold true otherwise.

$$c \equiv \frac{1}{CR}(\theta(t) - \theta_a) + \frac{P}{C} (°C/h) \quad (7)$$

$$r \equiv -\frac{1}{CR}(\theta(t) - \theta_a)(°C/h) \quad (8)$$

Equations (7) and (8) express the cooling (c) and heating rates (r) respectively, Malhamé & Chong [27] approximated the stationary solution of the CFPE assuming that the above rates are independent of temperature. Callaway [21] instead solved the CFPE eigenvalue problem to find the exact solution. An important observation at this point is that the rates are practically linearly dependent on the temperature difference, also steady ambient (θ_α) temperature in time is assumed.

One of the key contributions of this paper is increased insight in the importance of human behaviour in the operation of TCLs and subsequently aggregated behaviour of TCLs' population. Moreover, a new model is developed for that purpose which describes an individual TCL realistically. Our results suggest that clustering TCLs based on appliance parameters (R, C, P) will not result in homogeneous or relatively homogeneous populations, an essential assumption for most aggregation models and the developed control algorithms. Different clustering approaches and/or aggregation models need to be developed. The detailed bottom up MC model developed has high heterogeneity inherently, including the human factor, thus suitable for realistic DR simulations and to access the performance of aggregation models and control algorithms before real world experimental studies.

Section 2 reviews existing load models in literature and differences with real world data, Section 3 details our model and the human factor, Section 4 details Monte Carlo aggregation for heterogeneous populations (case study of cold loads), Section 5 presents our simulation results, and Section 6 concludes.

2. Real world data and TCL loads' population analysis

The original model, is suitable for "cold load pick-up", which is basically the response (demand) of TCLs after brown outs and/or black outs. The demand at that period may be assumed as the demand likely to occur in a similar given moment (date, day period, weather conditions), with a small "noise" factor for stochasticity. Even though this model is suitable to represent a "snap shot" of TCLs' population for a given moment (with knowledge of similar conditions, based on historic data), it doesn't reflect the dynamic nature of TCLs' population throughout the day, as well as the main driving factors behind this behaviour. As seen in some of these studies, the aggregated profile has significant differences with actual demand profiles. The best showcase being the cold loads, which are plugged in 24 h a day, where their aggregated demand is displayed as an almost straight line with a small fluctuation (noise). In reality, throughout the day, cold loads' aggregated demand is not almost linear, but rather seems to follow the trend of the rest demand, lower overnight and higher during the day, showing peaks around the same time as the total demand, in both residential and commercial cases. El-Férik & Malhamé [16] proposed an identification algorithm to calculate and update the parameters of the model, thus the model is able to cope with real world changes, with sampling intervals 15.198 min. or less. Assumptions of relatively steady ambient temperature (θ_α), small σ (practically no significant external disturbance) and homogeneity are required for this model.

In Fig. 2 the daily mean cold load from real world measurements is shown [28,29]. There are significant deviations in daily cold loads, yet the majority of the test cases used in the literature do not take that into account; e.g. in the Markov Chain aggregation used in Ref. [9], or the CFPE aggregation methods [21], which would normally change their statistic properties dynamically. The changes in consumption can be attributed to various factors [30], mainly
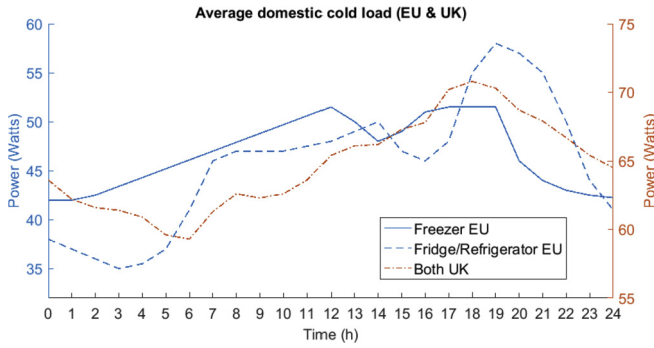
Fig. 2. Average measured daily demand of domestic cold loads, EU and UK, data sources: Smart-A [28], DECC [29].

ambient temperature changes and human interaction. Ambient temperature is the most important factor for cold loads [30], their contribution to the average domestic load is at least 36% in summer and 25% in winter, but there are big variations between households [13]. As observed in Fig. 2, early morning hours show a significant increase in mean fridge consumption, which can be attributed to human interaction (door opening) and heating when residents wake up.

The important note here is that **only part** of the population causes this increase, thus in reality that part has on average a higher increase than the mean displayed. It also varies between individuals. This is a good indication of the cold loads' population dynamics and how even identical appliances (homogeneous population characteristics) will behave differently due to external factors in time (heterogeneous population in operation, duty cycle). This is mainly due to human behaviour and the effect of human interaction on cold loads power consumption was studied in Refs. [30,31], where all concluded to it been the most important factor in energy consumption. The overall deviation in domestic demand (and behaviour) was studied in Ref. [32], which was based on a detailed model of domestic demand using real data from Time of Use Survey (TUS) [33], in order to keep human behaviour as realistic as possible. Fig. 3 shows two clusters (classification based) where there is an obvious difference in demand during working hours, as expected. This shows the clear difference in behaviour and human presence in households, as seen around working hours (9am − 7pm) there is distinct difference in demand around 150−200 W. The lowest demand for the second cluster (employed occupant) is attribute mainly to passive consumption of cold loads, with minimal to no interaction, whilst the first cluster shows human presence; interaction with appliances and most likely
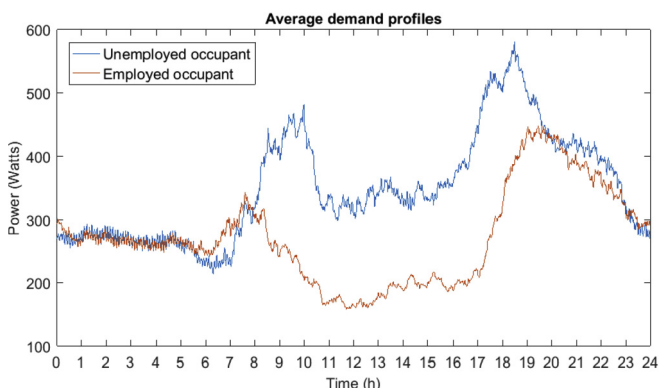
different household temperature (heating). As such cold loads' operation of even identical appliances (parameters R, C, P of Malhamé and Chong's model [27]) between these groups differ due to different ambient temperature and human interaction.

The aggregated power in (3) is not completely accurate, since it assumes that units on idle state consume no power. In reality most TCLs have a small consumption during idle state. Power demand is written more accurately as:

$$P_{total}(t) = \sum_1^N P_i(t) = \sum_1^N m_i(t) \cdot P_{on,i} + [1 - m_i(t)] \cdot P_{idle,i} \quad (9)$$

For a large enough number of loads N (Kolmogorov's law):

$$\overline{m} = 1/N \sum_1^N m_i(t) \rightarrow E(m(t)) \quad (10)$$

However, this can be assumed for homogenous or almost homogenous populations only. An operational characteristic of TCLs is the duty cycle (D), defined as the runtime ratio that a unit is on (t_{on}) within the period (T) of a cycle ($D = t_{on}/T$). Even though each TCL is either fully on or fully off, the probability to be on in random moment is equal to its duty cycle. The phase of the cycling of a TCL relative to another TCL is random, so for a large population the aggregate of all the individuals' demand tends to be independent of time. Given no external interactions or changes, the quasi-equilibrium condition is called the natural diversity of a cycling load. Thus based on these assumptions,

$$E(m(t)) = 1/N \sum_1^N D_i = \overline{D} \quad (11)$$

Equation (9) can be written as:

$$P_{total}(t) = \sum_1^N P_i(t) = N \left(\overline{D} \cdot \frac{1}{N} \sum_1^N P_{on,i} + [1 - \overline{D}] \cdot \frac{1}{N} \sum_1^N P_{idle,i} \right)$$
$$= N \left(\overline{D} \cdot \overline{P_{on}} + (1 - \overline{D}) \cdot \overline{P_{idle}} \right) \quad (12)$$

where $\overline{D}$ and $\overline{p}$ are the mean duty cycle and mean power rating respectively. The second part of (9) is the passive consumption of TCLs. In a population where duty cycle changes in time, $p_{idle,i}$ can be perceived as a constant base load and by introducing (13), (9) or (12) become (14)

$$P_i = P_{on,i} - P_{idle,i} \quad (13)$$

Fig. 3. Difference between 2 groups of domestic users [32].

$$P_{total}(t) = \sum_1^N P_i(t) = N \cdot \overline{D(t)} \cdot \overline{P} + P_{idle} \quad (14)$$

where P_{idle} the sum of $P_{idle,i}$. That base consumption is not affected by DR and thus can be disregarded in DR models as long as P_i is used instead of $P_{on,i}$.

Lastly a similar approach can be taken for a dynamic heterogeneous population. The first step is to create clusters of TCLs in time. Assume a number Z of clusters $C_j(t)$, whose population (z_j) and representative means are a function of time (15), then total consumption is approximated by (16), the larger the Z and the smaller the time steps the more accurate, but we also want to keep small number of clusters for computation efficiency but also larger population (m_j), thus higher statistical accuracy.

$$C(t) = \{C_1, C_2, \cdots, C_Z\} = g\{D(t), Z\} \qquad (15)$$

$$P(t) = \sum_{1}^{Z} \left[z_j \cdot \overline{D_j(t)} \cdot P_j(t) \right] + P_{idle}, \qquad (16)$$

As we can see, the population's demand is approximately linearly dependent on the duty cycle. Upon synchronization (e.g. a DR signal or power outage) this is no longer the case, synchronization causes units to operate simultaneously in phase and natural diversity will be re-established slowly in time due to heterogeneity and random factors or through corrective actions [21]. This synchronization causes the rebound effect and its magnitude is based on the number of synchronized units.

2.1. Non-linear consumption factors

The aim of this paper is to study the cause of the aggregated behaviour of TCLs and its effect on aggregated demand. Using main driving factors, create pragmatic models, which can be used to simulate real world scenarios of DSM and DR applications. A realistic model was created to incorporate the most important dynamics while also focusing on simplicity when possible, then validated against real world data from DECC [28] and Smart-A [29]. It was based on thorough and extensive research in experimental data of TCLs' model parameters [5,21], mainly on cold loads as a case study [8,20,34,35], thermal properties [30,31], human behaviour [30,31], and simulations. Additionally, on Laguerre's et al. thorough research which focuses on cold loads [36–38]. The model was created such that it may be used for either cold/cooling loads or heating loads. The governing Stochastic PDE (Partial Differential Equations) used can be applied to all normal thermal loads, with only the input changing. Cold loads were used for the base case study, being the best example but also the most common among TCLs, with the highest demand and potential for DR.

Important TCLs consumption factors and human in the loop:

a) Ambient temperature, a function of human behaviour and weather
b) Appliance characteristics and operation
c) Human behaviour, preferences and socio-economic factors

2.1.1. Ambient temperature

Thermal loads used by the industrial, commercial and residential sector make use of heat transfer mechanisms; advection, conduction, convection and radiation. For relatively small temperature changes, such as in the case of TCLs (domestic and commercial), Newton's law of cooling applies. Therefore, heat transfer and consecutively the thermal load is practically linearly dependent on the temperature difference,

$$\frac{d(\theta(t))}{dt} = -\lambda \cdot [\theta(t) - \theta_\alpha(t)] + m(t) \cdot Q_g \qquad (17)$$

where $m(t)$ defines the operational state of a TCL (1 for ON state and 0 for OFF/idle), λ constant (Newton's heat transfer coefficient), Q_g is the heat/cooling transferred during operation (ON state). As expected TCLs' energy consumption depends mainly on the ambient temperature and any change affects them directly, as seen in (7) & (8), cooling and heating rates are linearly dependent of $\Delta\theta$ ($\theta_{set} - \theta_\alpha$). Refrigeration demand during winter is about 2/3 of the one in summer, while there is also a deviation between daytime and night time [28,34]. Previous work on TCL modelling and simulations has assumed steady or relatively steady ambient temperature
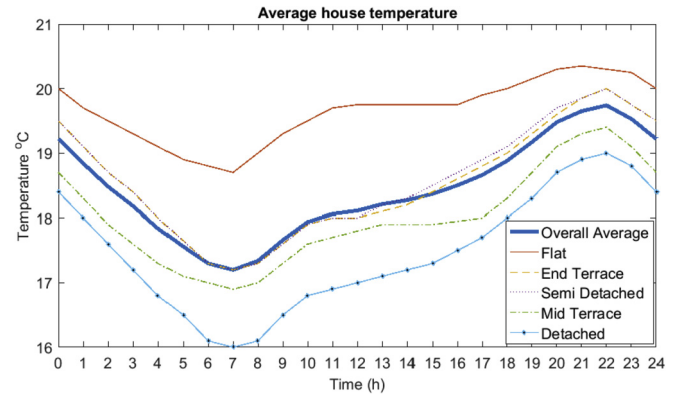

Fig. 4. Average temperature profile per house type, February 2010, 292 dwellings [39].

around a set value (i.e. [20–27]). In Ref. [39] variations of 10 °C in all house types during heating periods were found, which highlights the significance of θ_a in heterogeneity and deviation of heating practices. Zehir et al. [8], used real data to study cold loads' demand side management, where room temperature was also monitored, showing changes of 3 °C in a few minutes. Mean temperature during the day can be seen in Fig. 4, based on measurements over nine months for a UK city-wide survey of over 500 homes [39]. These are used as a reference of maximum, minimum and average temperature in the model developed. As discussed previously periods where there are ambient temperature changes for a part of the population are of significance to the accuracy of the load models.

An important note here is how equations (7)–(10) and (17) are linked. The thermal load or rather loss of it, is expressed by (17), which defines the cooling and heating duration (also rates in a population) and is linearly dependent of ΔT. Cooling and heating rates are also directly linked to duty cycle ($D = c/r + c$) [40]. Equation (18) is a natural outcome, since when the thermal demand changes power rating doesn't, what does is duty cycle, proportionally to the change of the thermal load. This is rather useful since it applies to aggregated populations too, thus knowledge of $D(t)$ (t_{on}, t_{idle}) through $P(t)$ can be used to estimate the state of a TCL, or with multiple reading across the whole population, a principle used in Ref. [16]. In Masjuki et al.'s measurements [30], energy consumption increased from 0.56 kWh/day to 1.12 kWh/day when the ambient temperature was raised from 16 °C to 31 °C, a 100% overall increase or equivalently around 37.3 Wh/day for a 1 °C increase in temperature. Hasanuzzaman et al. [31] has reported an increase in consumption from 1.2 kWh/day to 1.7 kWh/day, when ambient temperature was raised from 18 °C to 30 °C, 41.66% increase or 46 Wh/day per 1 °C. Therefore, for changes in short periods, such effects on state (D(t)) should be modelled.

$$\frac{d(\Delta\theta(t))}{\Delta\theta(t_0)} \cong \frac{d(D(t))}{D(t_0)} \cong \frac{d(P(t))}{P(t_0)} \qquad (18)$$

2.1.2. TCL characteristics and operation

During the operation of a TCL around the set-point value θ_{set}, there are θ_{min} and θ_{max} values which are the switching (ON/OFF) points. Excluding external interference, thermal losses are defined by the thermal characteristics of the appliance, namely thermal capacitance C, resistance R, efficiency η and also the difference of ambient θ_a and set-point temperature θ_{set} ($\Delta\theta$ as discussed above). Consequently, set-point temperature is of equal importance to ambient temperature. Set point actuation control algorithms are

based on the above fact (thermal load $\propto \Delta\theta$) [6,21,23]. The effect, as expected, is essential the same as ambient θ_α changes [30].

2.1.3. Human behaviour, preferences and socio-economic factors

Human behaviour, preferences and socio-economic factors vary across consumers and TCL end function. They are multi-variable dependent and stochastic, posing the biggest challenge to model, especially because they introduce heterogeneity in operation even among identical appliances, thus making a homogeneous population behave heterogeneously in time, directly affecting the accuracy of models and control actions. Yet for large populations, statistical approaches are fit for such tasks, especially given the fact humans are "creatures of habit", thus proper examination can lead to appropriate clustering and control frameworks. Each of these factors affect each load type differently and thus the examination breaks down per load type: space heating & cooling, water heating, cold loads.

Space heating/cooling loads operation is essentially a combination of weather and human behaviour. Human behaviour is rather complicated, being a function of three connecting variables; time, comfort zones (conditions, preferences) and socio-economic factors. For instance, a household of employed individuals, working office hours 9−5, is statistically less likely to use heating/cooling during office hours (individuals not present) on a given working day [32], Fig. 3 shows the difference in demand. Once a household is active (individuals present), heating/cooling might be used; it depends primarily on current conditions and individuals' preference of "comfort zones" but also socio-economic factors. De Cian et al. [41] examined the interaction between income, temperature and energy demand, where an income interaction model was created, examining the income/temperature elasticity of electricity demand. Additionally, in Kane T. et al.'s [39] work (real world measurements), the rebound effect was greater than expected, which is attributed to the above socio-economic behaviour. Thus geographical clustering for thermal loads, such as in Ref. [23] where relative homogeneity is assumed (air conditioners) and similar operation characteristics (θ_α) is inadequate, especially for TCLs such as colds loads. Water heating is similar, but less reliant on weather conditions or comfort zones, rather based on preferences and habits instead.

The major electric TCLs consumers, cold loads, have one external affecting factor, human behaviour. It can be broken down to door opening and loading the compartments. Experimental tests, using ISO standards [30], with door opening of 12 s at a 90° angle, report an increase in consumption from 0.85 kWh/day to 1.42 kWh/day, for 75 such events, 7.6 Wh (or 0.894%) increase per event. In practise, during door opening the insulation (and therefore overall heat transfer coefficient) change drastically, warm air mixes with cool air inside, heat transfer occurs through convection. A note at this point is that such events are dependent on $\Delta\theta$; it is the same $\Delta\theta$ during normal operation and during the event, with the change of overall heat transfer coefficient (h), thus the proportional increase (0.894%) can be assumed relatively constant given not high deviation of conditions. This can be expressed as:

$$\dot{Q}_{normal} = h_{normal}A(-\Delta\theta), \dot{Q}_{event} = h_{event}A(-\Delta\theta), \text{thus} \frac{\dot{Q}_{event}}{\dot{Q}_{normal}}$$

$$= \frac{h_{event}}{h_{normal}} \approx const$$

$$(19)$$

Experimental studies on refrigeration have actually showed that new load can have the greatest impact in consumption, especially in short term [30,31,37]. Zehir et al. [8] mention that these effects need to be considered during simulations, yet they are hard to
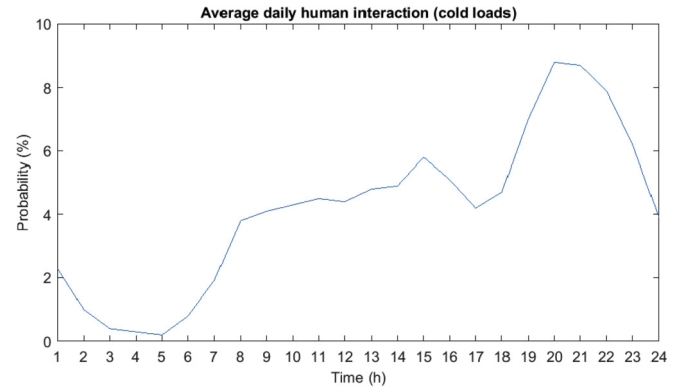

Fig. 5. Probability distribution of door-openings per day [29].

model. In Masjuki et al.'s measurements [30], energy consumption increased from 0.96 kWh/day to almost 2.3 kWh/day with 18 kg of water added (room temperature), though not linearly. Until about 9 kg the increase was linear, rate of about 37.5 Wh/kg, an increase of 3.9% per kg. Hasanuzzaman et al. [31] has reported an increase in consumption from 1.2 kWh/day to 1.9 kWh/day, with 12 kg of water added (room temperature), about 58.3 Wh/kg, increase of 4.83% per kg. Taking these findings into account, as well as the fact that those are not randomly distributed during the day (Fig. 5), it is obvious that a Wiener process (mean 0) with small variance (σ) doesn't properly model such effects or their impact in consumption and the TCLs populations' dynamic nature in time.

Moreover, (7), (8) do not include any of the above (θ_α, human interaction), since ambient temperature is assumed almost constant and the Wiener process isn't included due to having 0 mean and practically insignificant deviation. CFPE should have included this dynamic behaviour (heterogeneity) in time, thus some error is expected.

2.2. Population size and stochasticity

When dealing with stochastic approaches, population size is detrimental for statistical accuracy. Especially for realistic studies with heterogeneous populations, the number should be large enough to be able to model real world dynamics and have statistical validity. At the same time, we want to have the smallest possible acceptable size for computational efficiency. Relatively small population sizes might be also more appropriate to model and study commercial units, which have considerably higher demand than domestic loads but are also relatively limited in numbers (i.e. supermarkets refrigerators). In such a case bottom up models (such as Monte Carlo) are appropriate, others such as CFPE, Euler-Maruyama approximation etc. yield statistical errors, since the distribution of the population is Binomial.

At this point we will examine the model's population size. For highly heterogeneous populations, subject to external factors, it is hard to define a minimum acceptable population size. Yet, for the case of homogeneous, free of external factors TCL population, minimum population size can be calculated simply and efficiently through confidence intervals (CI). As previously mentioned, estimating available power in time is directly linked to estimation of the state of the population in that given time. It is thus essential to have a metric of the state in time, as well as a metric of its validity. The parameter that describes the state of an individual TCL (on/off probability) is its duty cycle $D \in (0,1)$. Based on above assumptions (homogeneous population, no external factors), this falls under a Bernoulli process, thus the Confidence Interval is directly linked to

the duty cycle and the size of the population.

The probability of each value x of a Binomial distributed random variable X is defined through its probability mass function:

$$X \cdot Bin(n,p) \leftrightarrow \Pr(X = k|n,D) = f(k; n, D) = \binom{n}{D} D^k (1-D)^{n-k} \tag{20}$$

Expected value: $E(X) = D \cdot N = \mu$, variance: $Var(X) = N \cdot Var(X_1) = N \cdot D(1-D)$

The above also holds true for heterogeneous populations when clustered in M relatively homogeneous clusters, where D is replaced by $\overline{D_i}$, $i \in (1, M)$. Taking into consideration the operational heterogeneity (D function of time for each individual), then clusters cannot be defined in a classic way, but rather dynamically in time blocks. In which case D(t) can be written for time blocks b = f(t), as D(b) and the above becomes:

$$\Pr_i(X = k) = f_i(k; N_i(b), D_i(b))$$
$$= \binom{N_i(b)}{D_i(b)} D_i(b)^k (1 - D_i(b))^{N_i(b) - k} \tag{20b}$$

The larger the population the closer to the expected value in a random moment, thus "random/uniform" distribution can be assumed with a small enough error. Confidence Intervals can be used as a metric; adjusted Wald, Wilson-Score, and exact Clopper-Pearson methods were considered. For large populations (n=> 1000) and .1 < p < .9, any of those 3 methods give practically the same results. For smaller populations the exact method is preferable.

The above values of duty cycle were selected since in reality cold loads' duty cycle fluctuates usually within this region. We can see that for populations (clusters) around 1,000, stochasticity is significant and their expected state wouldn't be as statistically accurate. The fluctuation introduced in the model due to being a binomial distribution will affect the accuracy of assessing the impact of the factors described above. For a population size of 100,000 it is well within limits and preferable, yet computationally slow. A model with size of 10,000 has acceptable accuracy to study TCLs' dynamics, whilst remaining computationally efficient. In a heterogeneous population, the above values are expected to change slightly. This can also serve as a metric for clusters' size (minimum requirements for statistical accuracy).

3. Realistic TCL modelling and human factor

3.1. Physically-based model of a single TCL

A TCL can be described by $\dot{\theta}(t) = -\lambda \cdot [\theta(t) - \theta_\alpha(t)] + m(t) \cdot q_g + u(t) \cdot q_e$

$$\tag{21}$$

Note that (21) is different to the classic one, as $\theta_\alpha(t)$ is not constant, and u(t), q_e represent interactions due to human behaviour, which in theory can be either positive or negative, most commonly in practise though, for cold loads positive, for water heating negative (use of water), for space heating either and space cooling positive. There is a definite difference between m(t) and u(t) since u(t) is stochastic.

3.1.1. TCL DE solutions (heating loads and cooling loads respectively)

$$\theta(t) = u(t) \cdot q_e \cdot (1/\lambda) + m(t) \cdot (1/\lambda) \cdot q_H + e^{-\lambda t} \cdot \left[\int \lambda \cdot e^{\lambda t} \cdot \theta_\alpha(t) dt \right] \tag{22a}$$

$$m(t) = \begin{cases} 1, \theta(t) < \theta_{set} - \dfrac{\delta}{2} = \theta_- \\ 0, \theta(t) > \theta_{set} + \dfrac{\delta}{2} = \theta_+ \\ m(t), otherwise \end{cases} \tag{22b}$$

$$\theta(t) = u(t) \cdot q_e \cdot (1/\lambda) + m(t) \cdot (-1/\lambda) \cdot q_C + e^{-\lambda t} \cdot \left[\int \lambda \cdot e^{\lambda t} \cdot \theta_\alpha(t) dt \right] \tag{22c}$$

$$m(t) = \begin{cases} 0, \theta(t) < \theta_{set} - \dfrac{\delta}{2} = \theta_- \\ 1, \theta(t) > \theta_{set} + \dfrac{\delta}{2} = \theta_+ \\ m(t), otherwise \end{cases} \tag{22d}$$

We introduce the parameter $\theta_g = (1/\lambda)q_H$ and $\theta_g = -(1/\lambda)q_C$ for heating and cooling accordingly, to simplify the above equations. θ_g can be perceived as the temperature gain (or loss for cooling), to which the system tends to during the on state (and would eventually approach for a prolong $t_{on}' \gg t_{on}$). At that point $\frac{d(\theta(t))}{dt} \sim 0 \rightarrow \theta(t_{on}') \cong \theta_g + \theta_a$. Similarly, $\theta_e = (1/\lambda)q_e$.

Equations (22a), (22c) can be written as:

$$\theta(t) = u(t) \cdot \theta_e + m(t) \cdot \theta_g + e^{-\lambda t} \cdot \left[\int \lambda \cdot e^{\lambda t} \cdot \theta_\alpha(t) dt \right] \tag{23}$$

3.1.2. Discrete solution

Solving (21) for discrete time steps (n to t) and using the same notations as above for θ_g, we get:

$$\theta(t) = \theta(n) e^{[\lambda(n-t)]} + [u(t)\theta_e + m(t)\theta_g] \left(1 - e^{[\lambda(n-t)]}\right)$$
$$+ e^{-\lambda t} \int_n^t \lambda \cdot e^{\lambda t} \cdot \theta_\alpha(t) dt \tag{24}$$

$$m_{(n+1)} = \begin{cases} 0, \theta_{(t)} < \theta_{set} - \dfrac{\delta}{2} = \theta_- \\ 1, \theta_{(t)} > \theta_{set} + \dfrac{\delta}{2} = \theta_+ \\ m_{(n)}, otherwise \end{cases} \tag{25}$$

3.1.3. At this point we will examine a fit for $\theta_\alpha(t)$ as a function of time

For space heating/cooling (heat pumps, air conditioners, electric space heating, gas heating), ambient temperature is perceived as the outdoors, which has relatively small variations from hour to hour and very small on a minute basis (the simulation time step). In

reality the change in external temperature depends on many factors and the best fit between small time steps is polynomial of small order or linear. For cold loads and water heaters, ambient temperature is indoors, which can have more sudden changes, such as early morning or when returning home and heat is turned on. The temperature increase in this case, based on experimental data seems to also follow polynomial or linear (Fig. 4 [39]). We will solve (23) and (24), difference is minimal thus linear is preferred for simplicity, if there is any case where $\Delta\theta_\alpha$ is significant (maybe in an industrial environment), the exponential one is a better fit though probably still of small importance. A note here is that the model is developed for a simulation time step of 1min, with temperature readings every 1 h, $\theta_\alpha(t)$ is thus fit to 1min steps through these.

3.1.4. Ambient temperature fit, $\theta_\alpha(t) = \alpha t + \beta$, continuous and discrete time solutions

The solution of the integral in (23), assuming linear fit, is:

$$[\alpha t + \beta - (a/\lambda)] \cdot e^{\lambda t} + C \tag{26}$$

Using (26), (23) is solved:

$$\theta(t) = \left[1 - e^{-\lambda t}\right]\left[u(t) \cdot \theta_e + m(t) \cdot \theta_g + \theta_\alpha(0) - (a/\lambda)\right] + \theta_0 \cdot e^{-\lambda t} + at \tag{27a}$$

or

$$\theta(t) = \left[1 - e^{-\lambda t}\right]\left[u(t) \cdot \theta_e + m(t) \cdot \theta_g + \theta_\alpha(0) - (a/\lambda)\right] + \theta_0 \cdot e^{-\lambda t} + \theta_\alpha(t) - \theta_\alpha(0) \tag{27b}$$

Discrete solution of (24) for $t = n + 1$ is (time step $l = t_{n+1} - t_n = 1$):

$$\theta(n+1) = \left[1 - e^{-\lambda}\right]\left[u(n) \cdot \theta_e + m(n) \cdot \theta_g - (a/\lambda)\right] + e^{-\lambda}\theta(n) + \theta_\alpha(n+1) - e^{-\lambda}\theta_\alpha(n) \tag{28a}$$

Adopting the notation $\gamma = exp(-\lambda)$ and replacing $\theta_\alpha(n+1) = a(n+1) + \beta = \theta_\alpha(n) + \alpha$:

$$\theta(n+1) = [1 - \gamma][u(n) \cdot \theta_e + m(n) \cdot \theta_H + \theta_\alpha(n) - (a/\lambda)] + \gamma\theta(n) + \alpha \tag{28b}$$

Equation (28b) can be rewritten as (28c) by replacing $[1 - \gamma][u(n) \cdot \theta_e]$ with $H(n)$ to simplify the effect of human interaction and keep the term separate. Comparing the above (both discrete and continuous) with the steady θ_α case (1), we can observe the dynamics of a non-constant θ_α (linear approximation).

$$\theta(n+1) = [1 - \gamma]\left[m(n) \cdot \theta_g + \theta_\alpha(n)\right] + \gamma \cdot \theta(n) + \alpha[\lambda - 1 + \gamma]/\lambda + H(n) \tag{28c}$$

The term $[\lambda - 1 + e^{-\lambda}]/\lambda$ defines the importance of α, which is the rate of change of the ambient temperature. This rate also depends on the time step, for larger time steps of θ_α (i.e. 10min instead of 1min), α has a value 10 times higher. $H(n)$ defines the effect of human behaviour, which as examined earlier has a considerable effect in cold loads consumption. It can be modelled to include a Wiener process though not mandatory when Monte Carlo simulation is used, since Monte Carlo introduces stochasticity. In this case a Wiener Process was deemed unnecessary since Monte Carlo introduced higher stochasticity and it would only be extra computational cost.

The model, similarly to (1), is composed of two interconnected subsystems, a linear part characterized by a stochastic continuous state $\theta(t)$, whose evolution depends on u(t) and a nonlinear part u(t) which changes states deterministically based on $\theta(t)$. This vector process $[\theta(t) \ m(t)]^T$ is a hybrid-state Markov process.

3.1.5. Constant $\theta_\alpha(t) = \theta_\alpha = const$, continuous and discrete time solutions

Practically these solutions are special cases of the above for $\theta_\alpha(t) = \theta_\alpha = cons$:

$$\theta(t) = \left[1 - e^{-\lambda t}\right]\left[u(t) \cdot \theta_e + m(t) \cdot \theta_g + \theta_\alpha\right] + \theta_0 \cdot e^{-\lambda t} \tag{29a}$$

$$\theta(n+1) = [1 - \gamma]\left[m(n) \cdot \theta_g + \theta_\alpha\right] + \gamma \cdot \theta(n) + H(n) \tag{29b}$$

These can be used for simplicity when θ_a is relatively constant or can be assumed as such based on the application.

3.2. Equivalent thermal models for multi-compartment TCLs

Fridge-freezers are the most common cold loads in households (about 69.7% ownership in 2014), whilst also being the cold load with the largest average consumption per unit [28] and are found in commercial buildings too. ISO 8187, ISO 8561, and ISO 7371 are the relevant standards for testing the energy consumption of household refrigerator−freezers having two or more compartments. At least one compartment (the fresh food storage compartment) is suitable for storing unfrozen food, and at least one compartment (the food freezer compartment) is suitable for freezing fresh food and for the storage of frozen food at −18 °C or lower [30,34]. They may be equipped with one or two compressors. In the case of one compressor, the operating cycle is controlled by both the refrigerator's and freezer's air temperature, while commonly a damper or fan is used to assist heat transfer from the refrigerator to the freezer. In the case of two compressors, each operating cycle is independent. The temperature in each compartment is better regulated but the price is higher, thus less common.

Deterministic equations governing temperature and operation state in each compartment are given by equation (30) for the case of one compressor and by equation (31) for the case of two compressors:

$$\dot{\theta}_f(t) = -\lambda_f \cdot \left[\theta_f(t) - \theta_\alpha(t)\right] - \lambda_{fr} \cdot \left[\theta_f(t) - \theta_r(t)\right] - u(t) \cdot q_C \tag{30a}$$

$$\dot{\theta}_r(t) = -\lambda_r \cdot [\theta_r(t) - \theta_\alpha(t)] + \lambda_{fr} \cdot \left[\theta_f(t) - \theta_r(t)\right] \tag{30b}$$

Adding (30a) and (30b):

$$\dot{\theta}_f(t) + \dot{\theta}_r(t) = -\lambda_f \cdot \left[\theta_f(t) - \theta_\alpha(t)\right] - \lambda_r \cdot [\theta_r(t) - \theta_\alpha(t)] - u(t) \cdot q_C \tag{30c}$$

Similarly, for the case of two compressors:

$$\dot{\theta}_f(t) = -\lambda_f \cdot \left[\theta_f(t) - \theta_\alpha(t)\right] - \lambda_{fr} \cdot \left[\theta_f(t) - \theta_r(t)\right] - u_f(t) \cdot q_{Cf} \tag{31a}$$

$$\dot{\theta}_r(t) = -\lambda_r \cdot [\theta_r(t) - \theta_\alpha(t)] + \lambda_{fr} \cdot \left[\theta_f(t) - \theta_r(t)\right] - u_r(t) \cdot q_{Cr} \tag{31b}$$

$$\dot{\theta}_f(t) + \dot{\theta}_r(t) = -\lambda_f \cdot \left[\theta_f(t) - \theta_\alpha(t)\right] - \lambda_r \cdot \left[\theta_r(t) - \theta_\alpha(t)\right]$$
$$- \left(u_f(t) \cdot q_{Cf} + u_r(t) \cdot q_{Cr}\right) \quad (31c)$$

Similar equations have been used by Keep et al. [24], (32) & (33), case of one compressor only, where they were discretized using Euler's method and simulated for a time step of 1 min, smaller time step simulations had no significant changes.

$$\dot{\theta}_f(t) = \frac{1}{mass_f \cdot c_f} \left[q_{of} + (q_c + q_a) - p\eta s\right] \quad (32)$$

$$\dot{\theta}_r(t) = \frac{1}{mass_r \cdot c_r} \left[q_{of} - (q_c + q_a)\right] \quad (33)$$

The main problem with modelling those as in [24], is the fact that they consist of 2 compartments with different set point temperatures and temperature dead-bands and as consequently different thermal dynamics ($\Delta\theta_{compartment-room}$). Therefore, the effects of θ_α change or human interaction are different. In both cases the operating cycles are determined by the compound dynamics of the system, and an equivalent (one compartment) simplified model of the system needs to be developed for computational purposes, to avoid slow simulation but also enable the use of a model as designed above. This becomes clear by looking (30), (31) or (32), (33), which after adding the stochastic elements of cold loads would be much harder to compute.

Note that in the case of two compressors on/idle states might differ, which means that the power consumption of the two differs in time. Yet, for an aggregated model of thousands of units, the percentage of units on is still directly linked to the duty (ἠ operating) cycle, consequently control of aggregated loads has statistically the same result.

The total thermal load losses of a refrigerator-freezer in static state (minimal to zero disturbance from external factors) is the sum of the freezer's and refrigerator's load, can be calculated as:

$$\dot{Q}_{tot} = \left(\dot{Q}_f + \dot{Q}_{f-r}\right) + \left(\dot{Q}_r - \dot{Q}_{f-r}\right) \quad (34)$$

where $\dot{Q}_f$ heat transfer from room to freezer, $\dot{Q}_{f-r}$ heat transfer from refrigerator to freezer and $\dot{Q}_r$ heat transfer from room to refrigerator. The heat transfer can be approximated as $\dot{Q} = hA(-\Delta\theta)$, where h is the heat transfer coefficient and A the surface respectively. The above equation can be written as:

$$\dot{Q}_{tot} = h_{f-room}A_{f-room}\left(-\Delta\theta_{f-room}\right)$$
$$+ h_{r-room}A_{r-room}(-\Delta\theta_{r-room}) \quad (35)$$

The equivalent single compartment model can be described by $h_{eq-room}A_{eq-room}(-\Delta\theta_{eq-room})$, where

$$A_{eq-room} = A_{f-room} + A_{r-room} \text{ and } h_{eq-room}$$
$$= w_f \cdot h_{f-room} + w_r \cdot h_{r-room} \quad (36)$$

The objective now is to find the θ_{eq}. Where w weight factors of compartment capacity to total capacity.

$$w_{fr} + w_{ref} = 1 \quad (37)$$

The two compartments share two dimensions, meaning that capacities are proportional to A, thus:

$$h_{eq-room}\Delta\theta_{eq-room} = w_{fr}h_{fr-room}\left(\Delta\theta_{fr-room}\right)$$
$$+ w_{ref}h_{ref-room}\left(\Delta\theta_{ref-room}\right) \quad (38)$$

Heat transfer coefficients are the sum of the internal cabinet coefficient (h_{fr}, h_{ref}) and the appliance's outside surface coefficient with the room (h_{room}). Studies have shown a difference less than 9% between freezer's and refrigerator's heat transfer coefficients (convective plus radiative), by adding the surface's coefficient the sums' difference is less than 4% (3.7%) [31]. The heat transfer coefficients can be set as:

$$h_{f-room} = (1-e)h_{r-room} \text{ or } h_{r-room} = (1+f)h_{f-room} \quad (39)$$

For simplicity h_{f-room}, h_{r-room} will be written as h_f, h_r for the following equations.

Using (36), (38) & (39) on (35) gives:

$$\theta_{eq} = \left(\theta_f \cdot w_f + \theta_r \cdot w_r - e \cdot w_f \cdot \theta_f\right) / \left(1 - e \cdot w_f\right) \quad (40a)$$

$$\theta_{eq} = \left(\theta_f \cdot w_f + \theta_r \cdot w_r + f \cdot w_r \cdot \theta_r\right) / (1 + f \cdot w_r) \quad (40b)$$

It is important to note that the aim of this equivalent model is to simulate the effects of external factors on energy consumption and the non-linear aggregated demand of cold loads. Typical values are given in Table 3, for different types of fridges. Approximations are used for simplicity and computational efficiency; in reality thermal laws have a different effect. As we can see in Fig. 6, the heat transfer is essentially always from the room to the freezer, directly or indirectly (through refrigerator), thus for normal operation the thermal behaviour is practically closer to the freezer's thermal properties. Yet human interaction with the refrigerator, i.e. door opening, extra load etc., will have an effect (heat transfer) closer to the refrigerator's thermal properties.

An examination of the above can be done with the experimental measurements in [31]. Using (18), in this case duty cycle change

Table 1
Confidence Intervals (0.95 & 0.98) for 1/3 duty cycle.

D = 0.333 (p)	CI 95%			CI 98%		
Population size	Low	High	MoE (%)	Low	High	MoE (%)
1000 (exact)	303.8	363.2	8.77%	298.6	368.8	10.39%
10,000 (adj. wald)	3241	3426	2.76%	3224	3444	3.30%
100,000 (any)	33041	33630	0.87%	32988	33677	1.03%

Table 2
Confidence Intervals (0.95 & 0.98) for 1/2 duty cycle.

D = 0.50 (p)	CI 95%			CI 98%		
Population size	Low	High	MoE (%)	Low	High	MoE (%)
1000 (exact)	468.5	531.5	6.30%	462.8	537.2	7.44%
10,000 (adj. wald)	4902	5098	1.96%	4884	5116	2.32%
100,000 (any)	49690	50310	0.62%	49635	50365	0.73%

Table 3
w_f and w_r values.

Freezer compartment (w_f)	Refrigerator (w_r)	
0.33	0.67	[24]
0.27	0.73	[30]
0.36	0.64	[31]
0.35	0.65	[36]

Table 4
Comparison of relative Power increase to relative Temperature increase.

Specifications [31]		Operation	
Power rating	165 W	Ambient 18 °C	1.2 kWh/day
Freezer weight factor (w_f)	0.282	Ambient 30 °C	1.7 kWh/day
Refrigerator weight factor (w_f)	0.718	$d(P)$ (%)	41.66%
Freezer (θ_{min}, θ_{max}) θ_{set}	(−21.5, −12) −16.75	$\Delta\theta$eq at 18 °C	20.043
Refrigerator (θ_{min}, θ_{max}) θ_{set}	(1.5, 5.5) 3.5	$\Delta\theta$eq at 30 °C	32.043
Equivalent thermal model θeq_{min}	−6.573	$d(\Delta\theta eq)$ (%)	55.53%
Equivalent thermal model θeq_{max}	−0.643	$d(\Delta\theta r)$ (%)	82.75%
Equivalent thermal model θeq_{set}	−3.608	$d(\Delta\theta f)$ (%)	34.53%

Table 5
Cold load data (experimental).

t_{on}	t_{idle}	cycle	θ_-	θ_+	θ_a	Duty cycle	P (W)	Ref
25′	75′	100′	3.5 °C	7 °C	20 °C	0.25		R[36,38]
30′	65′	95′	2 °C	5 °C	20*	0.316		R[20]
70′-140′	110′-110′	180′-250′	4.5 °C	7.5 °C	21	0.389−0.56		R[8]
30′	60′	90′	4 °C	8 °C	20*(a)	0.33		M[37]
34′	66′	100′	0 −22	7 −15	33 °C	0.34	197	M[35]
12′	36′	48′	3.5 −22	6.5 −11	20*	0.25		M[34]
28′*	65′*	93′*	1.5 −21.5	5.5 −12	18 °C	0.30**	165	M[31]
32′*	64′*	96′*	2.1 −19.1	4.3 −16.9	25 °C	0.33**	175	M[24]
30′	60′	90′	4 °C −31	8.2 °C −15	20 °C	0.33	120−160	M[36]
2 compressors (b)			−27	−17				F[36]

*data inferred or assumed based on similar experiments and loads **calculated from consumption and power rating.

 a Laguerre's experimental data in [37], but not referring exact ambient temperature as in [36,38]. Similar conditions are expected since it's the same climate and environment as the others.
 b Freezer with separate compressor running its own cycle [36].

Table 6
Cold load λ, θ_g (calculations).

| Cold load type	Ownership (%)	λ (20%)	θ_g (20%)	at θ_a	D
Refrigerator [36,38]	24.48%	3.179×10^{-3}	−58.815	20 °C	0.250
Refrigerator [20]		2.805×10^{-3}	−52.172	20*	0.316
Refrigerator [8]		1.458×10^{-3}	−38.541	21	0.389
Refrigerator [37]		4.795×10^{-3}	−41.856	20*(1)	0.333
Freezer [36]	30.46%	3.987×10^{-3}	−125.701	20 °C	0.333
Fridge (equiv.) [35]	45.06%	2.909×10^{-3}	−107.401	33 °C	0.340
Fridge (equiv.) [34]		7.102×10^{-3}	−87.323	20*(UK)	0.250
Fridge (equiv.) [31]		4.249×10^{-3}	−71.512	18 °C	0.301
Fridge (equiv.) [24]		1.202×10^{-3}	−85.819	25 °C	0.333
Fridge (equiv.) [36]		5.812×10^{-3}	−71.123	20 °C	0.333
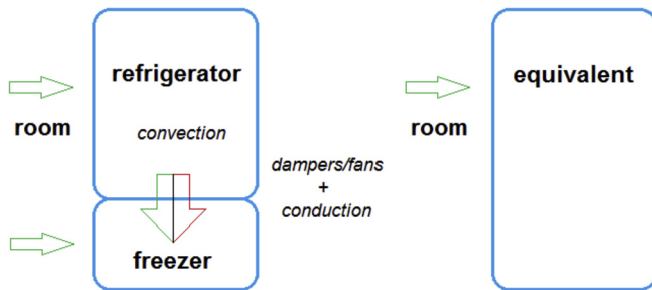
Fig. 6. Thermal model of a common fridge with 2 compartments (on the left) & the equivalent thermal model to be used for aggregation and DR (on the right).

from 0.303 to 0.429, or $\frac{d(D(t))}{D(t_0)} = 0.4158, \frac{d(D(t))}{D(t_0)} \approx \frac{d(P(t))}{P(t_0)} = 0.4166$, a difference less than 0.2%. Table 4 shows the relative consumption (P) and temperature (θ) increase.

4. Aggregation methodology and heterogeneity

Even though the simulations of CFP partial differential equations are much faster than the Monte Carlo ones and the accuracy satisfactory (under conditions), Monte Carlo is a bottom-up detailed model, better suitable in assessing the above developed model, where not all CFPE's conditions are met. Additionally, the aggregation process for CFP partial differential equations is more difficult and the complexity is higher, while also losing accuracy in heterogeneous models. The major advantage of Monte Carlo-based techniques is flexibility, as well as the highest possible accuracy in this case of highly heterogeneous populations with human behaviour, but also effective with smaller population sizes.

A note here is that defrost heater power and cycles are ignored for simplicity. Defrost heaters are typically on for less than 5% of the time [8,24], yet their demand during this time is usually considerably higher than that of the cold load's operation (480 W [8]). They

operate a few times per day, with daily consumption around 0.35 kWh [8] and are more suited as deferrable loads (non-dispatchable DR) rather than as flexible (dispatchable DR, though they can be used as both). They don't follow the models described in this paper, whose focus is a realistic model to represent the dynamics of TCLs (mainly cold loads as a test case) for dispatchable DR. The aggregated model flowchart is illustrated in Fig. 7.

4.1. Step 1: calculation of basic TCLs' parameters using experimental data

In [20] and [25], parameters such as appliance's thermal conductance, thermal mass, power consumption, coefficient of performance were used to determine the values λ, θ_g (Q_g) of (14). Those are constant, dependent on appliances' characteristics and independent of ambient temperature and human interaction. Hence simply knowing λ, θ_g is enough to build (14), an accurate representation of a TCL's physical model, a principle used in [16] where an algorithm was developed to identify them through readings of duty cycle (D).

Using values from Table 5, λ, θ_g can be calculated. During a deterministic cycle (without external effects) and constant (θ_α) ambient temperature, a TCLs idle cycle is described by

$$\theta(t) = \left(1 - e^{-\lambda t}\right)\theta_\alpha + \theta_0 \cdot e^{-\lambda t} \tag{41}$$

For $t = t_{idle}$: $\theta(t_{idle}) = (1 - e^{-\lambda t_{idle}})\theta_\alpha + \theta_0 \cdot e^{-\lambda t_{idle}}$. Case of cooling cycle, $\theta(t_{idle}) = \theta_+, \theta_0 = \theta_-$, substituting on (41) and solving for λ gives:

$$\lambda = -\frac{1}{t_{idle}}\ln[(\theta_+ - \theta_\alpha)/\theta_- - \theta_\alpha)] \tag{42}$$

$$\text{Similarly,}\, \theta_g = \left[\left(\theta_- - \theta_+ \cdot e^{-\lambda \cdot t_{on}}\right)\Big/1 - e^{-\lambda \cdot t_{on}}\right] - \theta_a \tag{43}$$

The values of [8] have significant variations compared to the rest; as stated by the authors, data was taken from a G class top mounted refrigerator, and was chosen as a good example for a low efficient refrigerator with high energy demand (relatively older model). According to Residential Energy Consumption Survey 2009, in USA, this was one of the most common (more than 60% percent) refrigerators in households, thus chosen by the authors for their study on 2009, also mentioning that customers mostly use the same appliance for more than 5 years up to 14 years. Newer models (post 2009) though are more efficient and more similar to those used in [20]. Similarly, for fridges (refrigerator-freezer) some of the above have significantly different conditions than what commonly observed in UK (i.e. 33 °C room temperature) or missing data. For the case of UK specifically, values from [20,31,36,38] are more suitable for a realistic model.

These are used via Monte Carlo to construct heterogeneous populations of TCLs (3 basic types of cold loads in this case) with randomized variance in parameters θ_g, λ, θ_α, and initial conditions θ (t), u(t); u(t) based on on/off probability which is equal to the duty cycle D of each. The population's mixture, as a percentage of each cold load type, is based on UK ownership statistics [28]. Specifically, for UK ownership of cold loads per household is about 107% (expressed to overall population), which means that 7% have an extra unit.

4.2. Step 2. Human interaction

The effect of human interaction as discussed in section 2 is relative to $\Delta\theta$ similarly to ambient thus better expressed in (%). We need to link that to the term H(b) of (20b), which varies for each type of load. To the best of the authors knowledge this is the first realistic human interaction modelling based on experimental data, such as measured effects of door openings or increased consumption per kg of extra load, combined with real data of frequency of human interaction. The exact procedure, in more detail can be seen in Fig. 8. Effectively, human interaction increases t_{on} or reduces t_{idle}. Using the fact that increase in consumption is linked to increase in duty cycle $\frac{d(D(t))}{D(t_0)} \approx \frac{d(P(t))}{P(t_0)}$ (18), we can express an increase in consumption by x (%) as an equal increase in duty cycle: $D' = D(1 + x)$.
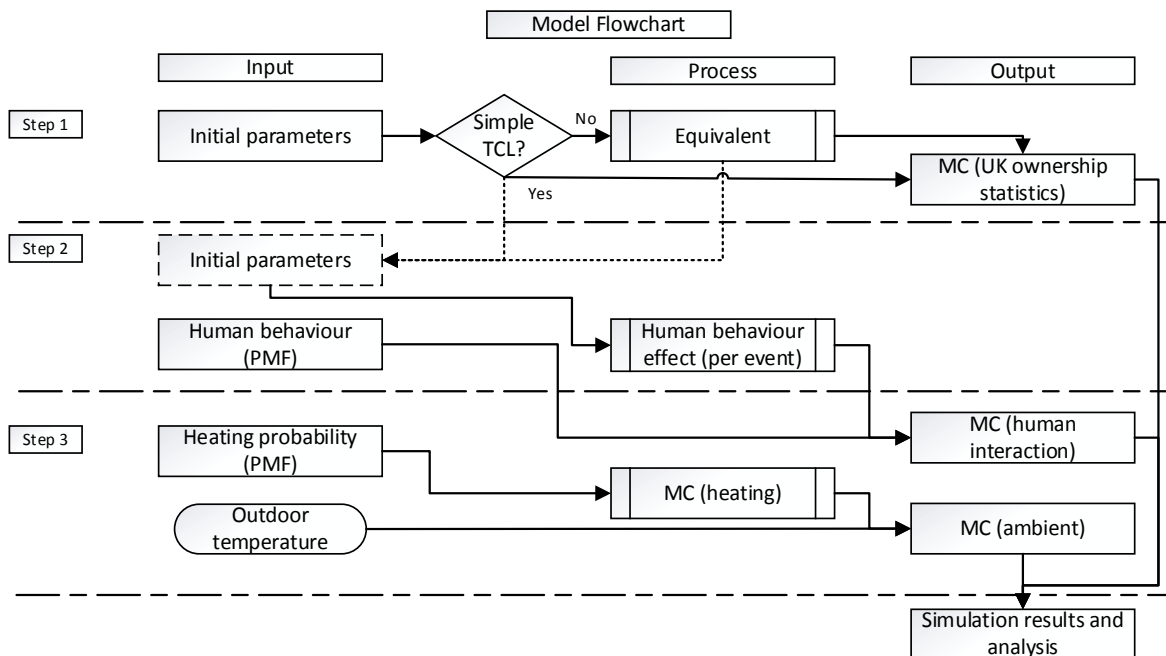

Fig. 7. Model flowchart.

Step 2: Human interaction

Input	Process	Output

Step 1

Initial parameters → Hb per load type (per event)

Effect per event (%)

→ MC (human interaction)

Step 2

Human interaction (PMF) → MC (events, minute resolution)
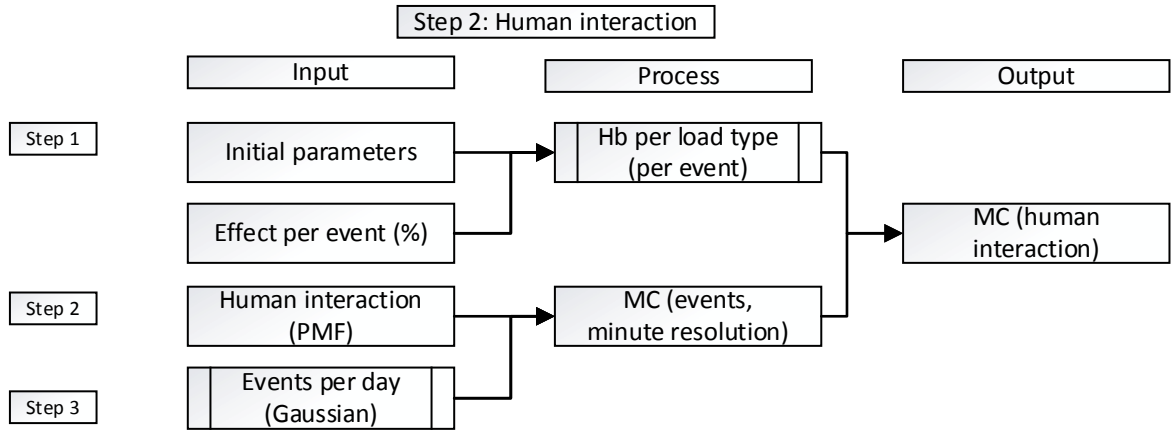
Step 3

Events per day (Gaussian)

Fig. 8. Human interaction modelling in detail (Step 2 of above flowchart).

We got thus the following two cases:

$$D' = \frac{t'_{on}}{t'_{on} + t_{idle}} = \frac{t_{on}(1+\varepsilon)}{t_{on}(1+\varepsilon) + t_{idle}} = \frac{t_{on}(1+x)}{t_{on} + t_{idle}} \tag{44}$$

$$D' = \frac{t_{on}}{t_{on} + t'_{idle}} = \frac{t_{on}}{t_{on} + t_{idle}(1-\zeta)} = \frac{t_{on}(1+x)}{t_{on} + t_{idle}} \tag{45}$$

The solutions to the above are:

$$\varepsilon = x\frac{t_{on} + t_{idle}}{t_{idle} - x\cdot t_{on}} \tag{46}$$

$$\zeta = x\frac{t_{on} + t_{idle}}{t_{idle}(1+x)} \tag{47}$$

We need to express H(b) as a function of those, assuming an event during t_{idle}, it can be described by:

$$\theta(t) = \left[1 - e^{-\lambda t}\right]\left[u(t)\cdot\theta_e + m(t)\cdot\theta_g + \theta_\alpha\right] + \theta_0\cdot e^{-\lambda t} \tag{48}$$

Using $[1 - e^{-\lambda t}][u(t)\cdot\theta_e] = H(t)$, (48) is written as: $\theta(t) = (1 - e^{-\lambda t})\theta_\alpha + \theta_0\cdot e^{-\lambda t} + H(t)$

For $t = t_{idle}$: $\theta(t_{idle}) = (1 - e^{-\lambda t_{idle}})\theta_\alpha + \theta_0\cdot e^{-\lambda t_{idle}} + H$, assuming H represents the accumulated effect during that time. In the case of a cooling cycle, $\theta(t_{idle}) = \theta_+$, $\theta_0 = \theta_-$:

$$H = (\theta_+ - \theta_a)\left[1 - \left(\frac{\theta_+ - \theta_a}{\theta_- - \theta_a}\right)^{-\zeta}\right] \tag{49}$$

similarly during ton:$H = (\theta_- - \theta_a - \theta_g)\left[1 - \left(\frac{\theta_- - \theta_a - \theta_g}{\theta_+ - \theta_a - \theta_g}\right)^\varepsilon\right]$ (50)

Using the above and experimental data described in Section 2 [30,31], human behaviour effect per event for each cold load type is calculated, separately for door opening and new load. Then using the frequency of door-openings per day, as described in [29] (see Fig. 5 in Section 2) an hourly PMF (probability mass function) is created, and a Gaussian distribution for events per day with expected mean 40–60 events and new load per day [30]. Those are used to create a Monte Carlo model with minute resolution for events per household throughout the day (Figs. 9–11). Events are based to reflect experimental ones, such as in [30], "door remained open for 12 s at an angle of 90°", but since one such event might
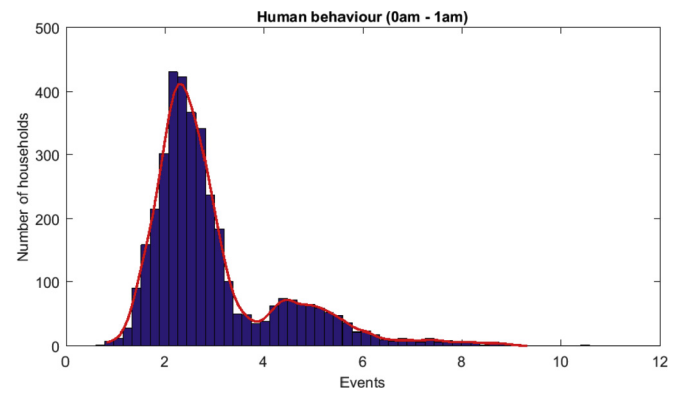
Fig. 9. Human interaction events: distribution between 0am and 1am for 10,000 households. A single event equals to "door remained open for 12 s at an angle of 90°" [30].

differ in reality (i.e. longer duration than 12 s), non-integer values were used (i.e. reflect the extra effect of an event with longer duration). Monte Carlo events are linked to the term Hb through (36), (37), (39) & (40) to express the effect in cold loads' state, consequently cycles and consumption.

4.3. Step 3. Ambient (room) temperature

Temperature fluctuations as discussed in Section 2 affect the state of TCLs directly, especially rather fast changes, such as those occurring in early morning and evening after work. Kane T. et al. [39] examined the variation of indoor temperatures and heating practices in UK dwellings, variation of up to 10 °C were reported, we use UK heating practise (probability of human behaviour essentially, as developed in model [39]), reported "preferred" comfort zones and outdoors temperature to create a realistic MC model. The heating PMF is used to create a Monte Carlo model of possible heating on action, which is then compared to probable indoor temperature (based on outdoor temperature) and thus hourly temperature is defined per dwelling. In reality, based on knowledge of weather conditions and historic data (population's behaviour to these conditions) the temperature can be probabilistically estimated. The resulting MC model is then converted to minute resolution. It could also be used in hourly resolution, with the term of (28c) α converted to hourly changes (in this case would be 60 times higher). Temperature changes in dwellings due to use of heating can occur in shorter periods than an hour [8], but for this model more "mild"
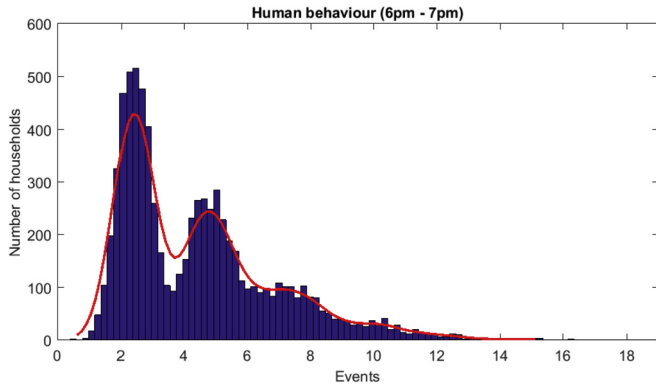
Fig. 10. Human interaction events: distribution between 6pm and 7pm for 10,000 households. A single event equals to "door remained open for 12 s at an angle of 90°" [30].
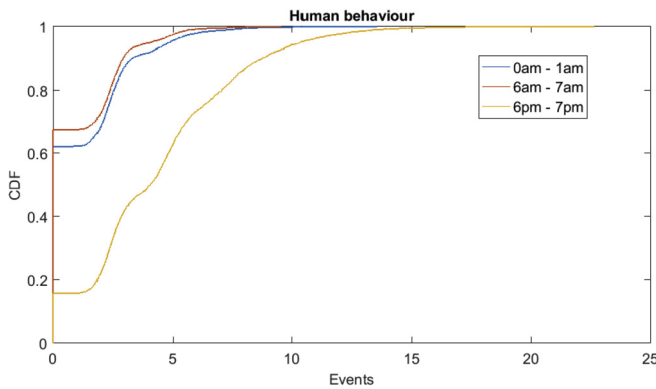

Fig. 11. Cumulative distribution of human interaction events. Comparison of different hours. As expected, 6am−7am has the minimum interaction, whilst 6pm−7pm has the highest.
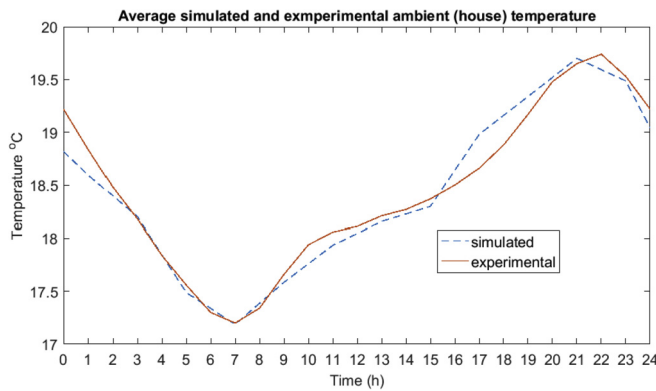

Fig. 12. Mean house temperature simulated (MCMC) for 10,000 units and UK data (Fig. 4 [39]).

fluctuations were used to describe the general behaviour of the population. Simulated average household temperature and reported average temperature ([39]) can be seen in Fig. 12, as expected they are very close. Assuming that this report is a good representation of UK's heating practises overall, the cold load demand is also expected relatively close to the actual report in [28].

5. Simulation results

One important aspect of a model described by (28c) is that it can focus on the state of the TCLs specifically without the power
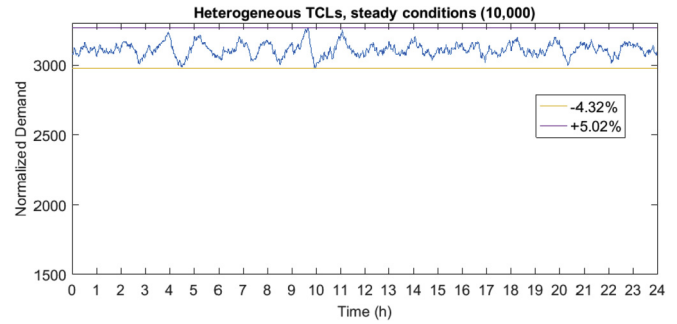

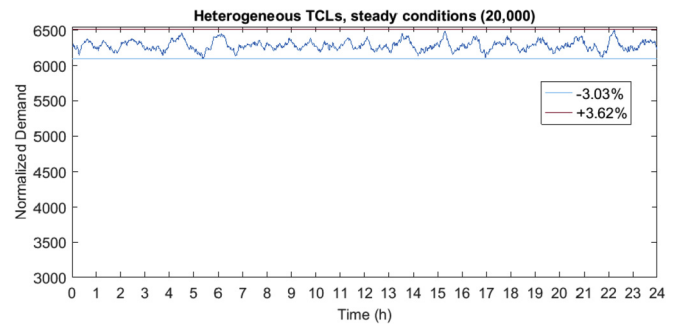**Fig. 13.** TCLs' population state without external factors.

Fig. 14. TCLs' population state without external factors.

demand of each. Thus, it can give a clear picture of TCLs' state and how they respond to different commands as well as other factors. Demand can be added through (9) to determine the total power demand of the TCLs' population.

The model can be used as classic models (Malhamé and Chong), by assuming θ_α constant and minimal external factors (Wiener process with mean 0 and small variance σ). In which case the heterogeneity of the population due to technical parameters can be studied and the effects of stochasticity. Figs. 13 and 14 show the difference between population sizes of 10,000 and 20,000. As expected the stochastic behaviour reduces as the population size increases, the values (fluctuation) are close but higher than those in Tables 1 and 2, due to heterogeneity. Populations of smaller size will have significant elements of stochasticity (i.e. 1000) and thus are not proposed for DR studies of TCLs. Unless the study is specifically aimed for small populations, then one of the most important elements to be studied is stochasticity and control actions need to take it into account. Increasing the population size from 10,000 to 20,000 has a small improvement, in this study a population of 10,000 was deemed satisfactory for examining effects of human interaction and ambient temperature. Assumptions of almost uniform distribution (around 1% fluctuation or less) for probabilistic models in large heterogeneous populations, require population sizes at the order of 100,000.

Detailed bottom up models, like this one has the highest fidelity study these behaviour characteristics. Arguably, one of the other important uses of this model is the realistic representation of TCLs under different conditions during the day and their dynamic behaviour in time. Especially when considering the human factor. Fig. 15 displays simulation results for varying ambient (room) temperature and human behaviour, as described in steps 2 and 3. It is also compared to experimental data from DECC and Smart-A as seen in Fig. 16 (converted to hourly means and experimental data scaled for comparison purposes). The difference with the "state of
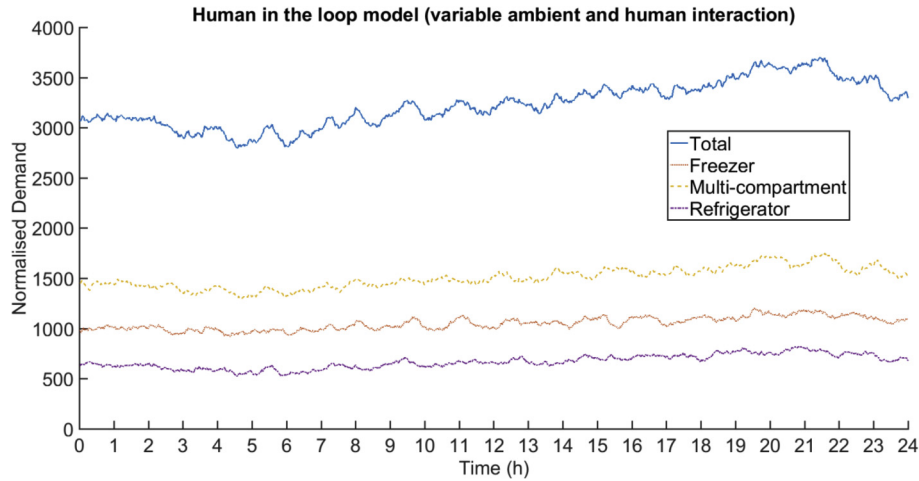
Fig. 15. . Realistic cold load demand simulation with external factors and human in the loop.
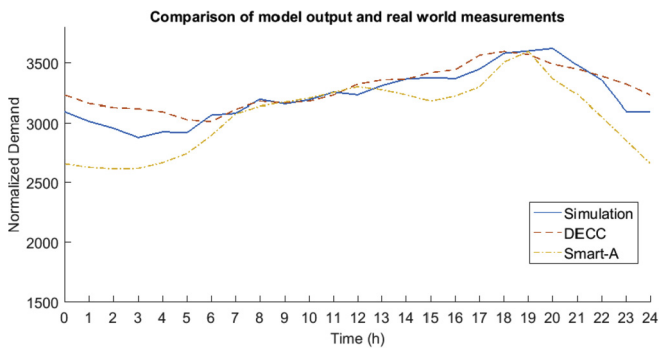

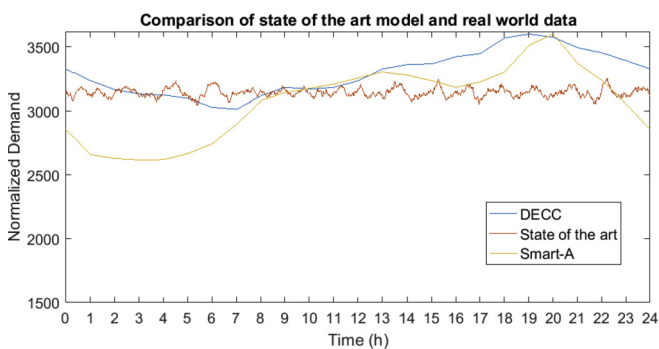**Fig. 16.** Comparison of simulated model and experimental data.

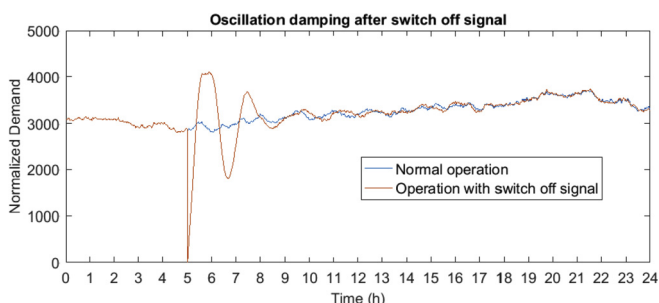**Fig. 17.** Comparison of "state of the art" model and experimental data.

Fig. 18. Switch off at t = 300' (and partial synchronization of TCLs).

the art" TCL model can be observed in Fig. 17.

Other important characteristics and phenomena that can be studied in detail with this model are the behaviour in external commands during different conditions (periods of the day), rebound effects and oscillation damping after those, due to partial synchronization (Figs. 18 and 19). The exact response of a DR actions (or other forms of interruptions such as brownouts), as shown below, are directly affected by TCLs aggregated state at that given period. Additionally, as these cause part of the TCL population to synchronize, rebound effects occur, which are detrimental for DR actions. They can be significant for dispatchable and non-dispatchable DR. For instance, when a certain amount of power is required for frequency control, TCLs can provide it by reducing demand output equal to that required amount, but after some time when the rebound effect is introduced an almost equal extra amount of energy is required, which if not countered properly by additional control actions could practically recreate the original problem [20].

It is thus essential for control actions to take such effects into consideration and try to minimize/counter them or at least post-pone them, as well as consider the natural damping occurring due to heterogeneity [21]. It is crucial to note that, in non-intrusive actions (thermal limits are maintained), the overall thermal load remains essentially the same. Consecutively, the electrical demand is also the same, but allocated in time, unless the control framework is designed otherwise.

One of the starting arguments of this paper and motivation for this work was whether small heterogeneity can be assumed for TCLs, such as cold loads, and the accuracy of models based on such assumption. Fig. 20 shows the variation of duty cycles during the day for 4 TCLs with relatively similar starting duty cycle (and thus operation), yet there is significant change during the day. This is true for the majority of the population, and the original point, that even in a (relatively) homogeneous population there will be sig-nificant heterogeneity in operation in time holds true, as well as that Wiener process with small variance is probably inadequate for representing it. This model can be used for detailed DR studies of TCLS, rebound effects, efficiency of control algorithms being a bottom up MC realistic model. Moreover, it is realistic point of reference to check the feasibility of models with less computational requirements (such as CFPE models) and their accuracy, which will be used in aggregators [21]. It is also important to note that response to control actions varies during the day (i.e. night-morning hours have relatively shorter cycles than evening), based on the state of the TCLs' population, also a factor in identifying the
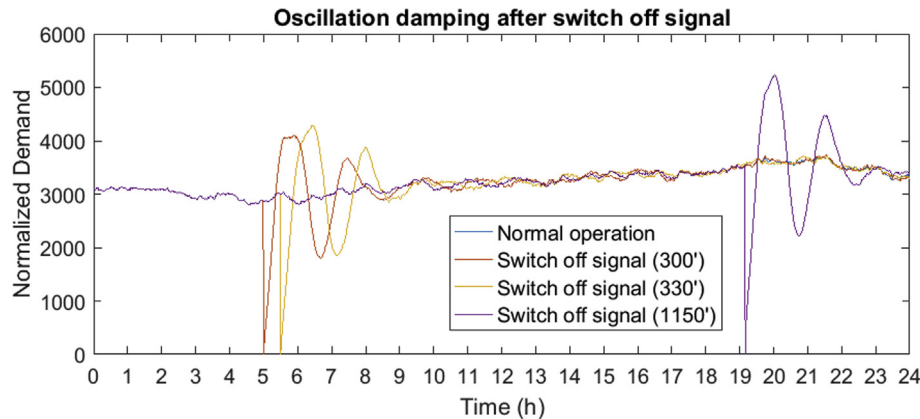
Fig. 19. Comparison of switch off actions at different conditions (moments). The higher the current demand the higher the rebound effect and its oscillations.
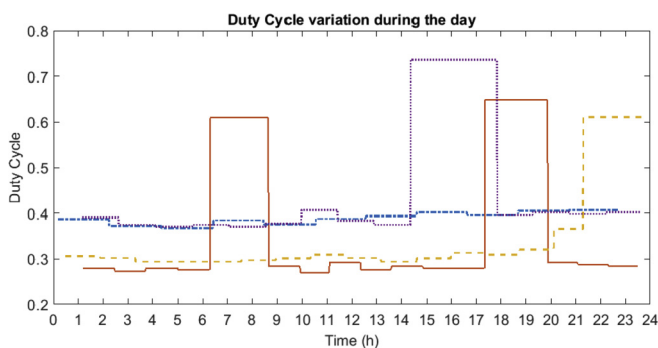

Fig. 20. Duty cycles of 4 randomly selected individuals during the day.

available power for DR.

6. Conclusions and future work

TCLs modelling was examined, and a detailed bottom-up realistic model was developed for DR studies, including human interaction modelling and its effect. Controlling large amounts of loads is inevitably only possible through probabilistic models, but also accurate enough. One of the keys issues for TCLs' applications is the high heterogeneity and the dynamic behaviour in time. Future work will focus on exploring solutions to this problem, potentially clustering frameworks as well as the impact of DR. Other important topics are computationally efficient aggregation models, control frameworks and data requirements for those.

This paper focuses on data from experimental studies to determine the most important factors in TCLs' dynamic behaviour. Based on those and the developed model, simulations were carried out for the case of colds loads. The initial hypothesis of high heterogeneity in operation even among relatively homogeneous loads was shown to hold true, thus the accuracy of various existing aggregation models is questionable.

Important points and outcomes can be summarized in 6 points (with DR significance order). First, showing the dynamic nature of TCLs and how their duty cycle (operation) changes during the day significantly, thus the problematic nature of using aggregation models such as CFPE by assumptions of relative heterogeneous groups. This is due to external factors, essentially human behaviour, which were modelled and simulated using real world data to highlight their actual effects in TCLs' consumption, subsequently also in TCLs' population state and thus DR. Additionally a simplified equivalent thermal model of multi-compartment cold loads was developed, which converts the actual second order thermal model to a first order one, thus useable for the S-PDE models developed so far for DR without loss of realistic TCLs characteristics. The bottom up approach used, can be computationally demanding due to its detail, yet that detail allows for high flexibility and the highest possible accuracy to study DR actions, rebound effects, test the performance of control algorithms. Additionally, it can be used to evaluate the accuracy of more computationally efficient aggregation models and simulate smaller populations taking into consideration the magnitude of stochasticity in such cases. Lastly, due to the main equations including external factors, minimum and maximum limits of "normal" operation can be deduced, as such abnormal (faulty) TCL consumption can be tracked, something useful mainly for commercial loads. So far this has mainly been done through regression models, but it can be used in conjunction to improve accuracy or to estimate accurately consumption under different operational conditions for energy efficient.

References

[1] Yousefi A, Nguyen TT, Zareipour H, Malik OP. Congestion management using demand response and FACTS devices. Int J Electr Power Energy Syst 2012;37(1):78–85.
[2] Lakshmanan V, Marinelli M, Hu J, Bindner HW. Provision of secondary frequency control via demand response activation on thermostatically controlled loads: solutions and experiences from Denmark. Appl Energy 2016;173: 470–80.
[3] Wang D, Parkinson S, Miao W, Jia H, Crawford C, Djilali N. Hierarchical market integration of responsive loads as spinning reserve. Appl Energy 2013;104: 229–38.
[4] Mathieu JL, Koch S, Callaway DS. State estimation and control of electric loads to manage real-time energy imbalance. IEEE Trans Power Syst 2013;28(1): 430–40.
[5] Managan K. Demand response: a market overview. Institute for Building Efficiency of Johnson Controls Inc; 2014.
[6] Callaway DS, Hiskens IA. Achieving controllability of electric loads. Proc IEEE 2011;99(1):184–99.
[7] Yao L, Lu HR. A two-way direct control of central air-conditioning load via the internet. IEEE Trans Power Deliv 2009;24(1):240–8.
[8] Zehir AM, Bagriyanik M. Demand Side Management by controlling refrigerators and its effects on consumers. J Energy Conv Manag 2012;64: 238–44.
[9] Mathieu JL, Callaway DS. State estimation and control of heterogeneous thermostatically controlled loads for load following. In: 2012 45th Hawaii international conference on system science (HICSS). IEEE; 2012, January. p. 2002–11.
[10] Koch E, Piette MA. Architecture concepts and technical issues for an open,

interoperable automated demand response infrastructure. Lawrence Berkeley National Laboratory; 2008.

[11] Woo CK, Kollman E, Orans R, Price S, Horii B. Now that California has AMI, what can the state do with it? Energy Pol 2008;36(4):1366–74.

[12] Energy Information Administration. Residential energy consumption survey. Washington, DC: U.S. Dept. Energy; 2001. Tech. Rep.

[13] Palmer J, Terry N, Kane T. Further analysis of the household electricity survey-early findings: demand side management. London, UK: Department of Energy and Climate Change (DECC); 2013.

[14] Song KB, Baek YS, Hong DH, Jang G. Short-term load forecasting for the holidays using fuzzy linear regression method. IEEE Trans Power Syst 2005;20(1):96–101.

[15] Hong WC. Chaotic particle swarm optimization algorithm in a support vector regression electric load forecasting model. Energy Convers Manag 2009;50(1): 105–17.

[16] El-Férik S, Malhamé RP. Identification of alternating renewal electric load models from energy measurements. IEEE Trans Automat Contr 1994;39(6): 1184–96.

[17] Huang KY, Chin HC, Huang YC. A model reference adaptive control strategy for interruptible load management. IEEE Trans Power Syst 2004;19(1):683–9.

[18] Huang KY, Huang YC. Integrating direct load control with interruptible load management to provide instantaneous reserves for ancillary services. IEEE Trans Power Syst 2004;19(3):1626–34.

[19] Goel L, Wu Q, Wang P. Fuzzy logic-based direct load control of air conditioning loads considering nodal reliability characteristics in restructured power systems. Elec Power Syst Res 2010;80(1):98–107.

[20] Totu LC, Wisniewski R, Leth JJ. Demand response of a TCL population using switching-rate actuation. IEEE Trans Contr Syst Technol 2017;25(4): 1537–51.

[21] Callaway DS. Tapping the energy storage potential in electric loads to deliver load following and regulation, with application to wind energy. Energy Convers Manag 2009;50(5):1389–400.

[22] Koch S, Meier D, Zima M, Wiederkehr M, Andersson G. An active coordination approach for thermal household appliances—local communication and calculation tasks in the household. In: PowerTech, 2009 IEEE bucharest. IEEE; 2009, June. p. 1–8.

[23] Perfumo C, Kofman E, Braslavsky JH, Ward JK. Load management: model-based control of aggregate power for populations of thermostatically controlled loads. Energy Convers Manag 2012;55:36–48.

[24] Keep TM, Sifuentes FE, Auslander DM, Callaway DS. Using load switches to control aggregated electricity demand for load following and regulation. In: 2011 IEEE power and energy society general meeting. IEEE; 2011, July. p. 1–7.

[25] Wai CH, Beaudin M, Zareipour H, Schellenberg A, Lu N. Cooling devices in demand response: a comparison of control methods. IEEE Trans Smart Grid 2015;6(1):249–60.

[26] Mortensen RE, Haggerty KP. A stochastic computer model for heating and cooling loads. IEEE Trans Power Syst 1988;3(3):1213–9.

[27] Malhamé R, Chong CY. Electric load model synthesis by diffusion approximation of a high-order hybrid-state stochastic system. IEEE Trans Automat Contr 1985;30(9):854–60.

[28] Department of Energy & Climate Change and National Statistics. Energy Consumption in the UK, Last Updated July 2015. Available at: https://www.gov.uk/government/collections/energy-consumption-in-the-uk.

[29] Stamminger R, Broil G, Pakula C, Jungbecker H, Braun M, Rüdenauer I, et al. Synergy potential of smart appliances. 2008. Report of the Smart-A project.

[30] Masjuki HH, Saidur R, Choudhury IA, Mahlia TMI, Ghani AK, Maleque MA. The applicability of ISO household refrigerator–freezer energy test specifications in Malaysia. Energy 2001;26(7):723–37.

[31] Hasanuzzaman M, Saidur R, Masjuki HH. Effects of operating variables on heat transfer and energy consumption of a household refrigerator-freezer during closed door operation. Energy 2009;34(2):196–8.

[32] Kleidaras A, Kiprakis A. A roadmap for domestic load modelling for large-scale demand management within Smart grids. In: Wireless and satellite systems. Springer International Publishing; 2015. p. 33–47.

[33] Collin AJ, Tsagarakis G, Kiprakis AE, McLaughlin S. Multi-scale electrical load modelling for demand-side management. In: Innovative Smart grid technologies (ISGT Europe), 2012 3rd IEEE PES international conference and Exhibition on. IEEE; 2012, October. p. 1–8.

[34] Short JA, Infield DG, Freris LL. Stabilization of grid frequency through dynamic demand control. IEEE Trans Power Syst 2007;22(3):1284–93.

[35] Hermes CJ, Melo C. Assessment of the energy performance of household refrigerators via dynamic simulation. Appl Therm Eng 2009;29(5):1153–65.

[36] Laguerre O. Heat transfer and air flow in a domestic refrigerator. In: Farid Mohammed M, editor. Mathematical modelling of food processing; 2010. p. 445.

[37] Laguerre O, Flick D. Heat transfer by natural convection in domestic refrigerators. J Food Eng 2004;62(Issue 1):79–88.

[38] Laguerre O, Ben Amara S, Moureh J, Flick D. Numerical simulation of air flow and heat transfer in domestic refrigerators. J Food Eng 2007;81(Issue 1): 144–56.

[39] Kane T, Firth SK, Lomas KJ, Allinson D, Irvine K. Variation of indoor temperatures and heating practices in UK dwellings. 2011.

[40] Kalsi K, Chassin F, Chassin D. Aggregated modeling of thermostatic loads in demand response: a systems and control perspective. In: 2011 50th IEEE conference on decision and control and European control conference. IEEE; 2011, December. p. 15–20.

[41] De Cian E, Lanzi E, Roson R. The impact of temperature change on energy demand: a dynamic panel analysis (No. 2007.46). Fondazione Eni Enrico Mattei; 2007.